

Three-qubit exact Grover within the blind oracular quantum computation scheme

Cica Gustiani, David P. DiVincenzo

March 11, 2022

Abstract

Here we extend the concept of blind client-server quantum computation, in which a client with limited quantum power controls the execution of a quantum computation on a powerful server, without revealing any details of the computation. Our extension is to introduce a three-node setting in which an oracular quantum computation can be executed blindly. In this Blind Oracular Quantum Computation (BOQC), the oracle (Oscar) is another node, with limited power, who acts in cooperation with the client (Alice) to supply quantum information to the server so that the oracle part of the quantum computation can also be executed blindly. We develop tests of this protocol using two- and three-qubit versions of the exact Grover algorithm (i.e., with database sizes $4 \leq N \leq 8$), obtaining optimal implementations of these algorithms within a gate array scheme and the blinded cluster-state scheme. We discuss the feasibility of executing these protocols in state-of-the-art three-node experiments using NV-diamond electronic and nuclear qubits.

1 Introduction

While the promise of distributed quantum information processing was already foreseen in theoretical work many decades ago [5, 44, 13], we have finally entered a time when some of these ideas can be implemented in the laboratory [23]. With these developments, it is timely to look at the theoretical situation in a new light, and to evaluate what can be done with the currently very limited resources that are available.

In this paper we lay out a concrete plan for putting several new concepts in distributed quantum computing into action. Blind quantum computation [9] is an example of a protocol in which quantum physics gives unique security properties in a distributed computing setting. It is a client-server scheme, in which a client with limited computing power wishes to make use of a powerful server, but in such a way as to assure that the server is “blind”, i.e., not able to determine what computation the client is running, and

not able to come into possession of any intelligible input or output data for this computation. It has been shown that an adaptation of the technique of cluster-state quantum computation [38, 39, 36] can achieve client-server blind quantum computation, and one aspect of our work in this paper will be to lay out the possibilities for achieving this in a distributed quantum device involving diamond NV centers.

It has been standard for twenty years to use oracular algorithms as test cases for quantum computing implementations. We will adopt this approach here as well, but we propose, here and in a companion detailed paper [22], a new approach to integrating oracular computations into the client-server paradigm. In a distributed setting, it is meaningful to consider the oracle to be a distinct node of a network. In the case of the Grover quantum computation, this means a node in possession of an actual physical database. Thus we propose here, and explore for implementation, a three-party distributed computation setting: the client (Alice), who wants to know the answer to a database-lookup problem; the oracle (Oscar) who is in possession of this database, and is willing to reveal information about it to a server, but in a blinded fashion that will only be intelligible to Alice; and finally the server itself (Bob), in possession of a powerful quantum computer, with the capacity to receive remote qubits from Alice and Oscar, to perform entangling operations, and to broadcast the results of quantum measurements, under instructions from Alice and Oscar.

Of course, many experiments have achieved some implementation of the two-qubit Grover algorithm. For instance, [12, 28, 2] used the NMR technique, [8, 20] used trapped ions, [17] used superconducting qubits, and [46] used Abelian anyons (in a simulation). Moreover, [43, 10] demonstrated the algorithm with the one-way quantum computer [38, 39], computation scheme [9] was demonstrated in [4] with just four photonic qubits. But we believe that current developments in the quantum technology of distributed processing using remote NV centers [26, 23] make our three-party version of blind client-server quantum computation feasible for a full implementation study.

We can indicate precisely how this implementation can be achieved for the standard two-qubit Grover problem (and will do so in the final section), but we will primarily use the present study to analyse the implementation of scaled-up oracle problems. Thus, we will examine in detail the possible realizations of three-qubit Grover. It is already known that going from two to three qubits adds challenges for the implementation: two calls to the oracle are needed rather than one. In addition, the original Grover procedure does not give an error-free identification of the database state, except in the single case of the two-qubit case [17]. This problem was solved by subsequent modifications of Grover’s procedure [11, 25, 33, 30], and we take account in the present work of these modifications needed to make the database search an “exact” algorithm.

Given the various inconvenient features of three-qubit Grover — two oracle calls, lack of exactness, necessity for two-qubit gates at all stages of the algorithm — it is not surprising that there has been only a limited set of attempts to implement in the laboratory, and never in a distributed or blind setting. But [21] represented quantum circuits for different

number of queries, [45] illustrated implementation with cavity quantum electrodynamics, an experiment using NMR was performed in [41], and [21] demonstrated using trapped atomic ions [16]. However, to maintain the certainty in going from two-bit to three-qubit Grover, more complex gates are required. Only one experiment so far demonstrated the three-qubit exact Grover, which used a magnetic resonance system [31].

But as we show below, “three-qubit Grover” in fact encompasses a very large set of potential algorithms, and we explore these possibilities systematically here, with the objective of identifying the easiest implementations in the NV-center setting. The multiplicities of these Grover algorithms come in several forms. First, the number of database entries can be as many as $N = 2^3 = 8$, but it can be fewer. Each of the new cases $N=5, 6, 7$, and 8, is a separate problem, and we consider all of these here. While for $N = 8$ all of the three-qubit states are in use, for $N < 8$ only a subset are used; the exact choice of this subset is another variable that we have studied one by one.

There is a final variation of the algorithm that, to our knowledge, has not been exploited before. It is not necessary that the number of distinct entries in the database of Oscar be equal to the number of entries used in the quantum register. For example, suppose that Oscar has five database entries, A, B, C, D, and E. He and Alice may agree on an encoding in which A can correspond to marking either the three-qubit memory location 000 or 001, while the other four have a unique location, say $B \rightarrow 010$, $C \rightarrow 011$, $D \rightarrow 100$, and $E \rightarrow 101$. Then, if Alice’s final measurement reveals either 000 or 001, she infers that datum A is stored in Oscar’s database. The algorithm will also be successful even if Alice cannot reliably distinguish between the 000 and 001 outcomes, so long as they are reliably distinguished from the others. For this reason, we refer to this approach below as the “POVM strategy”.

We have also exhaustively optimized over possible POVM strategies. We find that the most economical three-qubit Grover algorithm to implement is in fact exactly the one that we have just given as an example! It is perhaps surprising that using $N=6$ with only five data is preferable to simply using $N=5$, but we find that the POVM freedom allows for reduction of the gate complexity of the implementation, and thus in the cluster state implementation.

An unfortunate message is that even this most economical case among all the three-qubit Grover algorithms is still much more resource intensive than the two-qubit Grover algorithm. This increase is modest in the number of physical qubits used (4 vs. 3), but very large in the number of gate operations and repeated re-use of physical qubits (approx. 10x more), and correspondingly large in its coherence demands. Thus, it appears that within the Grover family of algorithms, a large jump in the implementation is unavoidable. To make these jumps smaller, it will be necessary to look at other families of oracle algorithms.

2 Preliminaries

2.1 One-way quantum computer and universal blind quantum computation

In this section two measurement-based quantum computation schemes — some of our works are based on these schemes — are recalled: the one-way quantum computer (1WQC) [38] and the universal blind quantum computation (UBQC) [9]. In principle, UBQC allows a client with small quantum power to delegate her private computation to an untrustworthy server; the server is a one-way quantum computer, namely a cluster state computer.

By contrast to conventional quantum computation, viz. the gate model, a computation within the 1WQC scheme is performed by *adaptively* measuring a cluster state. Adaptive means that the measurement basis can be dependent on previous measurement outcomes. Therefore, in the 1WQC scheme, a *cluster state* defines the quantum computer, and consecutive measurements define quantum operations. A cluster state is represented as an open graph \mathcal{G} , together with a set of input nodes I and a set of output nodes O , where I and O may intersect. The non-input nodes can be interpreted as qubits whose states are set in the xy -plane of the Bloch sphere; the initialization of the input nodes are determined by the quantum algorithm. The edges of the graph \mathcal{G} correspond to CPHASE gates operated on the corresponding node qubits. The measurements are parameterized with angles $\vec{\phi}$; the measurement operators are in the form $\{|+\phi\rangle\langle+\phi|, |-\phi\rangle\langle-\phi|\}$, where $|\pm\phi\rangle := \frac{|0\rangle \pm e^{i\phi}|1\rangle}{\sqrt{2}}$, and $\phi \in [0, 2\pi)$. From this point on, we refer to “measure in angle ϕ ” as a projective measurement in basis $|\pm\phi\rangle$. Henceforth, to represent such a computation, we express it as a set $\{(\mathcal{G}, I, O), \vec{\phi}\}$.

Since quantum measurements unavoidably introduce indeterminacy, adaptive measurements are performed to obtain deterministic quantum operations. A measurement angle ϕ_j can be X - or Z -dependent on outcome i , which means correcting ϕ_j to $(-1)^{s_i}\phi_j$ or $\phi_j + s_i\pi$ respectively. Here $s_i \in \{0, 1\}$ is the outcome of measurement i . This correcting scheme is nicely captured by the notion of *flow* [15], that is a map $f : I^c \mapsto O^c$ following certain criteria (A^c means the complement of set A). Thus, measuring j , $f(j)$ determines X correction and neighbors of $f(j)$ determine Z corrections.

Now Alice as a client wants to run her private quantum computation on the untrusted server of Bob, thus they run the UBQC protocol as follows. First, Alice has her computation in mind $\{(\mathcal{G}, I, O), \vec{\phi}\}$; she informs Bob only the graph’s form. She transmits her input qubits to Bob then transmits the rest of the qubits, which are the non-input nodes in \mathcal{G} , in the state $\{|+\theta_j\rangle\}$, $j \in I^c$, where $\theta_j \in [0, 2\pi)$ is randomly generated from a discrete set. Second, Bob entangles the received qubits according to the edges of graph \mathcal{G} by applying CPHASE gates. Third, Bob measures every node in \mathcal{G} in angle δ_j that is publicly announced by Alice, where $\delta_j := \phi_j + \theta_j + r_j\pi$, where $r_j \in \{0, 1\}$ is randomly generated. Bob announces every outcome b_j after measuring node j .

The key feature contributing to the blindness of UBQC is the randomness introduced into several of the variables: $\vec{\theta}$ which hides the measurement angles, and \vec{r} which hides the measurement outcomes. Since $\vec{\theta}$ is a vector of parameters describing a set of non-orthogonal quantum states, inferring $\vec{\theta}$ is impossible without disturbing the quantum states. Since \vec{r} is randomly generated and is independent of $\vec{\delta}$, knowing an actual measurement outcome $s_j := b_j \oplus r_j$ from $\vec{\delta}$ and \vec{b} is impossible. Thus, no information is gained by Bob during the protocol run without disturbing the quantum states.

2.2 The exact Grover-Høyer search algorithm

The optimality of the Grover algorithm is well known [47]; high success probability is achieved with the fewest iterations. As the number of items in the database N increases, the success probability approaches one, whereas for small N the error is appreciable. For instance, success probabilities (p_N) running 3-qubit Grover are: $p_5 = 0.968$ with 1 iteration, $p_6 = 0.907$ with 1 iteration, $p_7 = 0.871$ with 2 iterations, and $p_8 = 0.945$ with 2 iterations. Because of this problem, many workers devised modifications or generalizations of the Grover algorithm to achieve probability one. For instance, Høyer [25] introduced arbitrary phase rotation in quantum amplitude amplification, Chi and Kim [11] introduced the single query search for the case when one quarter of the database is marked, Long [33] improved Chi and Kim’s algorithm using a phase matching condition that works for databases with size 2^n , followed by Liu [30] who generalized it for an arbitrary size and combination of databases. This section provides details of the so-called *Grover-Høyer algorithm*, which combines previous Grover and Høyer procedures to achieve probability one — later we develop a new algorithm based on that, which also features oracle separation, blindness, and measurement freedom.

Suppose n qubits are used to represent all indices $x = \{0, \dots, 2^{n-1}\}$. One may arbitrarily choose N elements of x that represent indices of a database w , thus $w \subset x$, where $|w| = N$, and we will consider the case $2^{n-1} < N \leq 2^n$. Without loss of generality, we start from a product of zero states $|0\rangle^{\otimes n}$. We consider an operator A that maps a product state into an equal superposition of N states, thus $A|0\rangle^{\otimes n} = (1/\sqrt{N}) \sum_{j \in w} |j\rangle =: |\Psi_{in}\rangle$. Suppose we have marked items in the database $\tau \subset w$ — we are interested in a special case where $|\tau| = 1$, thus $\tau \in w$. Given an oracle that evaluates a function $f(j)$ that indicates if j indexes a marked item of database, f induces a partition in the Hilbert space into “solutions” (τ) and “non-solutions” ($w \setminus \tau$) subspaces. Rewrite the state $|\Psi_{in}\rangle = \sqrt{a}|\tilde{\Psi}_1\rangle + \sqrt{1-a}|\tilde{\Psi}_0\rangle$, where $a = 1/N$, where $|\tilde{\Psi}_1\rangle$ and $|\tilde{\Psi}_0\rangle$ are the normalized states corresponding to $|\Psi_1\rangle := \sum_{j \in \tau} |j\rangle$ and $|\Psi_0\rangle := \sum_{j \in w/\tau} |j\rangle$. Henceforth, we will work in the Hilbert space defined as the subspace spanned by basis $\{|\tilde{\Psi}_0\rangle, |\tilde{\Psi}_1\rangle\}$.

Using previously described variables, running [Algorithm 1](#) within database w will reveal the marked item τ with probability one. The main idea of the algorithm is to combine the Grover algorithm with Høyer’s arbitrary phase rotation (also known as Høyer amplitude amplification), which performs the necessary rotation to bring the state vec-

Algorithm 1 Grover-Høyer algorithm

Require: w, τ

(1) Classical processing

1: $N \leftarrow \text{size of } w$

Ensure: $2^{n-1} < N \leq 2^n$ and $\tau \in w$

2: $\theta_0 \leftarrow \arcsin(1/\sqrt{N})$

3: $m \leftarrow \lfloor (\frac{\pi}{2} - \theta_0)/2\theta_0 \rfloor$ number of Grover runs

4: $\theta \leftarrow \frac{\pi}{2} - 2m\theta_0$ the remaining rotation

5: $\psi, \varphi, u \leftarrow \text{Equation 4, Equation 5, Equation 6.}$

6: $A \leftarrow |\Psi_{in}\rangle \langle 0|^{\otimes n}$

7: $\{D(\pi), D(\psi)\} \leftarrow \text{Equation 2}$

8: $\{O(\pi), O(\varphi + u)\} \leftarrow \text{Equation 1}$

9: Obtain a set of necessary operators \mathcal{B} (Equation 3), which are expressed within operations that can be done with the corresponding quantum computer.

(2) Quantum processing

10: $|\Psi\rangle \leftarrow \mathcal{A} |0\rangle^{\otimes n}$

11: **for** $j = 1$ to m **do**

12: $|\Psi\rangle \leftarrow \mathcal{D}(\pi)\mathcal{O}(\pi)|\Psi\rangle,$

13: **end for**

14: $|\Psi\rangle \leftarrow \mathcal{D}(\psi)\mathcal{O}(\varphi + u)|\Psi\rangle$

15: Measure $|\Psi\rangle$

16: **Exit**

tor exactly into the solution space. The modified iteration introduces new operators $\{O(\varphi + u), D(\psi)\}$, where

$$O(\varphi) = -I + (1 - e^{i\varphi}) |\tau\rangle\langle\tau| \quad (1)$$

$$D(\psi) = -I + (1 - e^{i\psi}) |\Psi_{in}\rangle\langle\Psi_{in}|. \quad (2)$$

The algorithm comprises two stages: **classical processing**, where compatible set of operations for every required unitary is obtained:

$$\{\mathcal{A}, \mathcal{O}(\pi), \mathcal{D}(\pi), \mathcal{O}(\varphi + u), \mathcal{D}(\psi)\} =: \mathcal{B}, \quad (3)$$

and **quantum processing**, where the quantum computation is performed on the quantum computer; every operator in \mathcal{B} respectively correspond to unitary matrices in $\{A, O(\pi), D(\pi), O(\varphi + u)\}$. When we say that we have a compatible set of operations \mathcal{A} corresponding to the unitary operator A (and similarly for all elements of \mathcal{B}), we mean that we specify an explicit implementation of A as a sequence of operations \mathcal{A} that can be performed for some model of quantum computation, *e.g.*, in the form of quantum gates or operations on a cluster state. For instance, our result in Figure 3 works on a quantum computer which performs CNOT and arbitrary 1-qubit gates.

The Høyer amplitude amplification is described by an operator $Q(\varphi, \psi) = D(\psi)O(\varphi)$, which rotates a state closer to the solution space by as much as θ , where $|\sin(\theta)| \leq$

$\sin(2\theta_0)$, $\theta_0 = \arcsin(1/\sqrt{N})$. Høyer found φ and ψ such that $Q(\varphi, \psi)$ performs the desired rotation:

$$\psi = \arccos\left(1 - \frac{\sin^2(\theta)}{2a(1-a)}\right) \quad (4)$$

$$\varphi = 2 \arctan(\psi/2)(1-2a) \quad (5)$$

$$u = \arg\left(-a(1 - e^{i\psi}) - e^{i\psi}\right) - \arg\left((1 - e^{i\psi})\sqrt{a(1-a)}\right). \quad (6)$$

Using those angles, $Q(\varphi, \psi)$ rotates the state by angle θ up to some phases $\pm u$;

$$Q(\varphi, \psi) = \begin{pmatrix} 1 & 0 \\ 0 & e^{iu} \end{pmatrix} \begin{pmatrix} \cos \theta & -\sin \theta \\ \sin \theta & \cos \theta \end{pmatrix} \begin{pmatrix} 1 & 0 \\ 0 & e^{-iu} \end{pmatrix}. \quad (7)$$

The unwanted phases $\pm u$ can be cancelled by performing the sequence $P(-u)Q(\varphi, \psi)P(u)$, where $P(\alpha) = -I + (1 - e^{i\alpha})|\tau\rangle\langle\tau|$. Since the form of operator P is identical to that of O , $O(\varphi)P(u) = O(\varphi+u)$ (see step 14 of Algorithm 1). When Høyer amplitude amplification is applied in the last iteration of the Grover algorithm, the state is entirely aligned to the solution space after the application of $P(-u)Q(\varphi, \psi)$. Thus, applying $P(u)$ afterward will change only the global phase of the state. This is the reason for omitting the last phase correction in Algorithm 1.

2.3 Exhaustive search for most economical Grover algorithm

The challenge in realizing the Grover-Høyer algorithm — apart from running the quantum processing with arbitrarily small error — is the optimization of the circuit preparation indicated on line 9 of Algorithm 1, where the desired unitary map must be written out as a set of quantum gates that can be run in the quantum computer. We develop an approach based on DiVincenzo and Smolin [18] (DS94) to overcome this challenge — such a challenge will appear again later when we need to obtain a graph state. This section mainly reviews DS94.

DS94 is a systematic, exhaustive approach: given the desired unitary map M , where $M \in \text{SU}(8)$, a set of 2-qubit gates networks are optimized over, where every 2-qubit gate is in $\text{SU}(4)$. We refer to “topology” of a 2-qubit gate network as a configuration of those 2-qubit gates. As we are concerned here with a 3-qubit operations, as was also the case in the study of DS94, the notations of DS94 are used: qubits are indicated with numbers 1, 2, and 3; a 2-qubit gate is indicated with the number of the untouched qubit. A topology is denoted by numbers within parenthesis, where each number represents the corresponding 2-qubit gate. So, for example, topology (321) indicates 2-qubit gates applied on qubits: $\{1, 2\}$, $\{1, 3\}$, and $\{2, 3\}$; note that the order of gates here is relevant, since these gates do not commute.

To efficiently obtain an exhaustive set of topologies, all possible topologies of 2-qubit gate networks are enumerated, then the equivalent ones are eliminated. Two different

topologies can be equivalent for the following reasons[18]: *time-reversal* which means placing the gates in time-reversed order, *e.g.*, $(12123) = (32121)$; *bit-relabelling* *e.g.*, relabeling qubit 1 and 2, thus $(12123) = (21213)$; and *conjugation by swapping* which means swapping of the states of any pair of bits, *e.g.*, $(12123) = (13123) = (12323) = (12313)$. For the systems with an unused subspace in the Hilbert space — thus for $N < 8$, where N is the dimension of the Hilbert space — the reordering must preserve the state space. For instance, database $w = \{0, 1, 2, 4, 7\}$ is conserved with permutation of every element in S_3 — this is easiest seen by writing this set w in three-bit notation, $w = \{000, 001, 010, 100, 111\}$. On the other hand, database $w = \{0, 1, 2, 3, 4\}$ is conserved only with one permutation of S_3 : $\begin{pmatrix} 1 & 2 & 3 \\ 1 & 3 & 2 \end{pmatrix}$.

The non-linear minimization Broyden-Fletcher-Goldfarb-Shanno (BFGS) [37] is used for the optimization in DS94 with the objective function defined as $f = \sum_i \sum_j |M_{ij} - S_{ij}|^2$, where M is the desired $SU(8)$ unitary, and S is the matrix resulting from composing the 2-qubit gate network. The minimization is over the parameters of the individual $SU(4)$ matrices describing the two-qubit gates. It is successful if $f = 0$ to a reasonable accuracy; thus a 2-qubit gate network that implements M is found.

3 Results

3.1 The blind oracular quantum computation scheme

Toward the realization of oracular computations within the client-server paradigm, while offering blindness as a security feature, we propose a quantum computation scheme called *blind oracular quantum computation* (BOQC). We give a sketch of the scheme here, with more mathematical details available in [22]. The scheme offers a solution in a setting with the following requirements: Alice is a client who wants to run an oracular quantum algorithm. Oscar is another client who is in possession of oracles and is willing to cooperate with Alice to run her oracular algorithm. Bob is a server who owns a powerful quantum computer on which Alice and Oscar can run the algorithm. But Bob is curious, and he is to be prevented (“blinded”) from acquiring knowledge of the algorithm or its output. For example, as previously illustrated, in a situation when Alice wants to run a Grover algorithm, Oscar is in the possession of database and helps Alice to discover the marked datum in the database by implementing the Grover oracle (or its Høyer variant), without leaking this information to Bob or to any other parties.

Running a computation within the BOQC scheme comprises the following steps. **First**, Alice and Oscar independently plan out their quantum computations within the 1WQC scheme. Alice will run the non-oracle blocks and Oscar runs the oracle blocks. Let Alice’s computation be $\{(\mathcal{F}, I, O), \vec{\Phi}\}$ with input nodes I and output nodes O , where \mathcal{F} comprises subgraphs $\mathcal{F} \equiv (\mathcal{F}_1, \dots, \mathcal{F}_p)$ together with the corresponding angles $\vec{\Phi} \equiv (\vec{\Phi}_1, \dots, \vec{\Phi}_p)$. Let Oscar’s computation be $\{\mathcal{G}, \vec{\phi}\}$, where \mathcal{G} comprises subgraphs $\mathcal{G} \equiv$

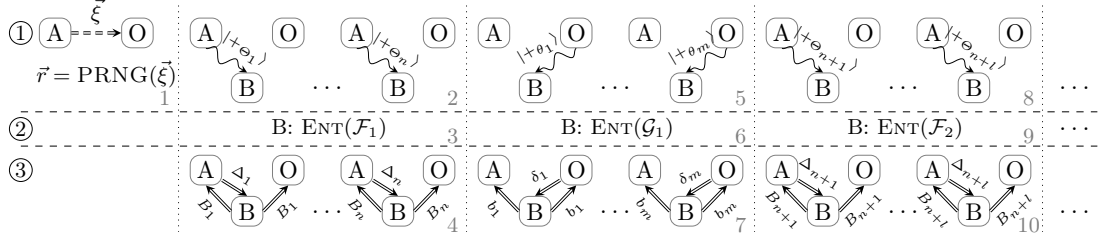


Figure 1: The BOQC and the optimized BOQC protocols. The initials A , B , O denote Alice, Bob, and Oscar respectively. The double dashed arrow in part 1 represents an authenticated channel — Alice sends Oscar a random key $\vec{\xi}$, which is then expanded to $\vec{r} = \text{PRNG}(\vec{\xi})$. Double solid arrows represent classical channels, over which variables $\{\Delta_j, \delta_k, B_j, b_k\}$ are sent. Wavy arrows represent quantum channels, where quantum states $\{|+\theta_j\rangle, |+\theta_k\rangle\}$ are transmitted; vector $\{\Theta_j\}$ is generated and known only to Alice and $\{\theta_j\}$ is generated and known only to Oscar. The vertical dashed lines separate subgraphs. The function ENT is an entangling operator performed by Bob applying CPHASE gates according to edges of the corresponding subgraph. The BOQC protocol is performed by following these steps: ① preparation, which comprises key sharing and qubit transmission, ② entanglement, which is the applications of entangling operations by Bob, and ③ measurement, where two-way classical interactions take place between clients and server; Bob measures each qubit in an angle instructed by Alice or Oscar, then he publicly announces the outcome. The optimized BOQC protocol comprises the same steps, however following the order that is notated by grey numbers.

$(\mathcal{G}_1, \dots, \mathcal{G}_q)$ together with the corresponding angles $\vec{\phi} \equiv (\vec{\phi}_1, \dots, \vec{\phi}_q)$. The total computation is $\{(\mathcal{T}, I, O), \vec{\Sigma}\}$, where $\mathcal{T} = (\mathcal{F}_1, \mathcal{G}_1, \mathcal{F}_2, \dots)$ with the corresponding angles $\vec{\Sigma} = (\vec{\Phi}_1, \vec{\phi}_1, \vec{\Phi}_2, \dots)$. Alice sends Oscar a random seed $\vec{\xi}$ via an authenticated channel to share a string \vec{r} , which is generated by both of them using a pre-agreed pseudorandom generator $\vec{r} = \text{PRNG}(\vec{\xi})$, where $|\vec{r}| \gg |\vec{\xi}|$. Then, Alice sends Bob input qubits, followed by Alice and Oscar alternately sending Bob the remaining qubits that correspond to non-input nodes. The non-input nodes are prepared in a specific way: Alice prepares $\{|+\theta_j\rangle\}$ and Oscar prepares $\{|+\theta_k\rangle\}$, where $\theta_j, \theta_k \in [0, 2\pi)$; $\vec{\Theta}$ are random angles known only to Alice and $\vec{\theta}$ are random angles known only to Oscar. **Second**, Bob entangles the received qubits by applying CPHASE gates that correspond to the edges of graph \mathcal{T} . **Third**, Bob measures all non-output nodes — if there is no quantum output for Alice, as in the Grover case, Bob measures all nodes. These measurements are performed one by one, where every angle is publicly announced: Alice announces $\Delta_j := \theta_j + \Phi_j + \pi r_i$ if qubit i corresponds to one of her nodes, Oscar announces $\delta_k := \theta_k + \phi_k + \pi r_i$ if qubit i is one of his nodes; Bob publicly announces his measurement outcome. If Alice expects quantum output, Bob sends her the output qubits in the end. Those steps are pictorially shown in [Figure 1](#).

Given that \mathcal{T} has a flow, running a computation within the BOQC while implementing

the UBQC correction scheme (see [Section 2.1](#)), will result in the same computation as if it is run within UBQC scheme, which is deterministic for all measurement angles and measurement outcomes. The proof of this statement is provided in [\[22\]](#).

If the physical qubits employed, which should have long coherence times, can be rapidly re-initialized, the BOQC protocol can be optimized to use fewer resources; this optimization is similar to the scheme in [\[24\]](#). Assuming that Bob’s qubits are reused after being measured, Alice and Oscar alternately perform a complete computation round; pictorially this means using the order denoted with gray numbers in [Figure 1](#), where the last layer of \mathcal{F}_j is left unmeasured, becoming the input of \mathcal{G}_j — thus, the last unmeasured layer of \mathcal{G}_j is the input of \mathcal{F}_{j+1} .

Further optimization can be done by partitioning \mathcal{F}_j and \mathcal{G}_j into smaller subgraphs, for instance, into subgraphs comprising the qubit about to be measured and its nearest neighbors. We demonstrate an algorithm computed within such an optimized BOQC scheme using NV centers ([Section 3.4](#)). The measurement corrections of such scheme is covered in [\[22\]](#).

We monitor the security of our protocol using the leaking function defined in [\[1\]](#). We observe that the BOQC protocol is blind while leaking only the graph structure \mathcal{T} . Recall Bob possesses information $\{\vec{\Theta}, \vec{\theta}\} =: X$ that are attributes of the quantum states and $\{\Delta, \delta\} =: Y$, where $\Delta_j = \Theta_j + \Phi_j + \pi r_i$ and $\delta_k = \theta_k + \phi_k + \pi r_i$. But the random quantities $\{\vec{\Theta}, \vec{\theta}, \vec{r}\}$ are independent of actual computation $\{\vec{\Phi}, \vec{\phi}\}$, thus X is independent of Y . Since X is encoded within quantum states, inferring $\vec{\Theta}$ or $\vec{\theta}$ without disturbing the quantum states is impossible. Thus, no information is gained by Bob during protocol run — the BOQC is blind.

The only catch in the security of BOQC is the establishment of the symmetric string \vec{r} between Alice and Oscar. We assume that Bob cannot learn about \vec{r} — Bob cannot learn the random seed $\vec{\xi}$ since we use an authenticated channel here. If Bob knows the function PRNG, guessing \vec{r} compromises the security with probability $2^{-|\vec{\xi}|}$. Thus, $\vec{\xi}$ must be long enough that the probability of Bob correctly guess the seed is infinitely small.

3.2 Construct circuits for Grover-Høyer algorithm

In this section, we present a strategy to obtain quantum circuits that run the Grover-Høyer algorithm. We will specifically explore cases where the database is encoded within three qubits, where $N = 5, 6, 7$, and 8 . The strategy essentially is seeking every circuit in \mathcal{B} ([Equation 3](#)) using DS94 optimization. The main challenges are the abundance of database choices and 2-qubit gate networks to be tried out; note that $\binom{8}{N}$ database choices are possible for each N . A strategy to group those choices into a small number of equivalent sets will also be presented here.

Algorithm 2 Circuit search

Require: w, τ

- 1: $l \leftarrow 0$
 - 2: $\mathcal{N} \leftarrow$ all unique topologies of 2-qubit gates network with size l
 - 3: **for** G in \mathcal{N} **do**
 - 4: Optimize G
 - 5: **if** the optimization succeeds **then**
 - 6: **return** G , the circuit is found and **Exit**
 - 7: **end if**
 - 8: **end for**
 - 9: $l \leftarrow l + 1$ and go to line 2
-

We seek quantum circuits using [Algorithm 2](#) — for $N \in \{5, 6, 7, 8\}$, for all unique database combinations w , and all marked items $\tau \in w$ — by finding all operations in $\mathcal{B}_{w, \tau}$ (see [Equation 3](#)), that is the required operators to run the Grover-Høyer algorithm for a database w and a marked item τ . Note that this search of circuits is done separately — one may do it for the whole Grover-Høyer algorithm and obtain smaller circuits — in order to obtain a BOQC-compatible circuit.

We will see that many database choices are equivalent by considering the role of the Grover oracle. For convenience, rewrite a database set $w = \{d_1, d_2, \dots, d_N\} \equiv d_1 d_2 \dots d_N$, where $d_j \in \{0, 1, 2, 3, 4, 5, 6, 7\}$. Given three bits $|ijk\rangle$ to encode w , where $i, j, k \in \{0, 1\}$, and a set of oracle operators where each of them “marks” one element by phase $e^{i\varphi}$. Two sets of database w_1, w_2 , where $|w_1| = |w_2|$, are equivalent if a set of oracles that can mark for all $\tau_1 \in w_1$ can also mark for all $\tau_2 \in w_2$ up to some global phases.

By this means, while considering their bit representations, w_1 is equivalent to w_2 if they are identical up to permutation and bit complementation. For instance, consider two equivalent databases with their bit representations (in little-endian format): $01234 = \{000, 001, 010, 011, 100\}$, $10543 = \{001, 000, 101, 100, 011\}$. One can be obtained from another by complementing the third bit and permuting the first and the second bits.

In the gate model, it means their oracles are equivalent up to some operations:

$$\begin{array}{c} \text{---} \boxed{O_{01234}} \text{---} \\ \text{---} \boxed{O_{01234}} \text{---} \\ \text{---} \boxed{O_{01234}} \text{---} \end{array} \equiv \begin{array}{c} \text{---} \times \text{---} \\ \text{---} \times \text{---} \\ \text{---} \times \text{---} \end{array} \begin{array}{c} \boxed{O_{10543}} \\ \boxed{O_{10543}} \\ \boxed{O_{10543}} \end{array} \begin{array}{c} \text{---} \times \text{---} \\ \text{---} \times \text{---} \\ \text{---} \times \text{---} \end{array}, \quad (8)$$

where O_{01234} and O_{10543} represents the oracle operators for databases 01234 and 10543 respectively. With these equivalences, all databases are covered by the following set:

$$\{01234, 01247, 01256, 012345, 012347, 012567, 0123456, 01234567\} =: \mathcal{D}. \quad (9)$$

Note that this strategy works for an arbitrary number of bits, not only for three.

As one may freely define a set of quantum gates that compose gate networks (for instance DS94 considered the set of all $U(4)$ matrices), we follow 1WQC and compose the gate

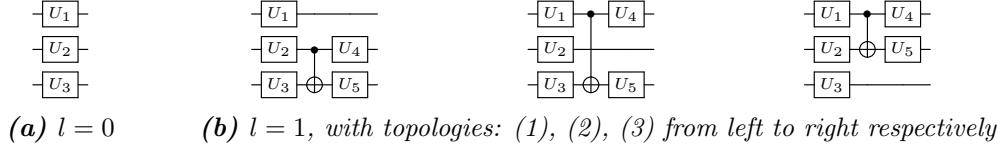


Figure 2: The distinct 2-qubit gate networks for $l = 0$ and $l = 1$. Operators $U_j \equiv U_j(\alpha_j, \beta_j, \gamma_j)$ are 1-qubit gates as in Equation 10.

networks into the operations $\{\text{CNOT}, U\}$, where U is a unitary matrix in $\text{SU}(2)$ having the form

$$U(\alpha, \beta, \gamma) = \begin{pmatrix} e^{i\beta} \cos(\alpha) & e^{i\gamma} \sin(\alpha) \\ -e^{-i\gamma} \sin(\alpha) & e^{-i\beta} \cos(\alpha) \end{pmatrix}, \quad (10)$$

where $\alpha, \beta, \gamma \in [0, 2\pi)$ are free parameters; these will be the optimization parameters below. We define l to be the number of CNOTs in our three-qubit network. For $l = 0$, the network is simply three 1-qubit gates; for every additional CNOT gate, four 1-qubit gates are added, two before and two after. Thus, $6l + 9$ free parameters will be available for the optimization for a network with size l . All networks for $l = 0$ and $l = 1$ are shown in Figure 2.

Again, not all networks are distinct; we obtain a minimal set of representative networks by enumerating all possible network topologies, followed by two eliminations: we eliminate ones that have more than three consecutive CNOT gates, and we eliminate the ones that are topologically equivalent [18] (also discussed in Section 2.3). The first elimination is based on the fact that an arbitrary $\text{SU}(8)$ can be constructed using three CNOT gates and eight 1-qubit gates [42]. Thus, for example, topology (133331) is eliminated since $(133331) = (13331)$.

We use DS94 optimization within Algorithm 2 to find the gate networks. A BFGS solver of the Python SciPy library [27] is employed in our program. To speed up optimizations, we define more relaxed objective functions than DS94:

$$f_b = \sum_{i,j \in w, M_{ij} \neq 0} |M_{ij} - S_{ij}|^2 \quad f_p = \sum_{i \in w, M_{i0} \neq 0} |M_{i0} - S_{i0}|^2, \quad (11)$$

where M is the desired unitary matrix and S is the resulting matrix from the tested network (G); f_p is used if $M = A$, that is the preparation block in $\mathcal{B}_{w,\tau}$, and f_b is used for other blocks in $\mathcal{B}_{w,\tau} \setminus \{A\}$. While the M s are assumed to be unitary matrices here, it is sufficient to consider only the non-zero elements within the subspace that is induced by w . Note that f_p is appropriate for $M = A$ because we start from the all-zero state $|0\rangle^{\otimes n}$.

Success in optimization is defined as $f_p \leq \varepsilon$ or $f_b \leq \varepsilon$, where ε is a chosen numerical precision. We define ε such that the success probability is approximately one: given δ , there exists an ε such that $p_s \geq 1 - \delta$, where p_s is the success probability of running Al-

(a) $N=5$, $\varphi + u=0.1707$, $\psi=0.4510$

w	\mathcal{A}	$O(\pi)$	$D(\pi)$	$O(\varphi + u)$	$D(\psi)$
01234	2	0 1 2 3 4	7	0 1 2 3 4	8
CNOT		1 1 1 1 0		2 2 2 2 0	
01247	2	0 1 2 4 7	7	0 1 2 4 7	8
CNOT		0 1 1 1 1		0 2 2 2 2	
01256	3	0 1 2 5 6	8	0 1 2 5 6	9
CNOT		0 1 1 1 1		0 2 2 2 2	

(b) $N=6$, $\varphi + u=1.861$, $\psi=0.841$

w	\mathcal{A}	$O(\pi)$	$D(\pi)$	$O(\varphi + u)$	$D(\psi)$
012345	1	0 1 2 3 4 5	4	0 1 2 3 4 5	6
CNOT		2 2 1 1 1 1		4 4 2 2 2 2	
012347	2	0 1 2 3 4 7	6	0 1 2 3 4 7	7
CNOT		2 1 1 2 1 1		4 2 2 4 2 2	
012567	3	0 1 2 5 6 7	8	0 1 2 5 6 7	8
CNOT		1 1 1 2 1 1		2 2 2 2 2 2	

(c) $N=7$, $\varphi + u=2.0277$, $\psi=1.2056$

w	\mathcal{A}	$O(\pi)$	$D(\pi)$	$O(\varphi + u)$	$D(\psi)$
0123456	3	0 1 2 3 4 5 6	8	0 1 2 3 4 5 6	9
CNOT		3 2 2 1 2 1 1		4 4 6 2 4 2 2	

(d) $N=8$, $\varphi + u=2.2143$, $\psi=1.5708$

w	\mathcal{A}	$O(\pi)$	$D(\pi)$	$O(\varphi + u)$	$D(\psi)$
01234567	0	0 1 2 3 4 5 6 7	6	0 1 2 3 4 5 6 7	6
CNOT		6 6 6 6 6 6 6 6		6 6 6 6 6 6 6 6	

Table 1: The number of CNOT gates for all distinct combinations of (w, τ, M) for all $w \in \mathcal{D}$, $\tau \in w$, $M \in \mathcal{B}_w$, and $N \in \{5, 6, 7, 8\}$. The angles φ, ψ , and u refer to the Høyer exact-Grover technique, see [Algorithm 1](#).

[Algorithm 1](#) while replacing block M with the tested network G . For the non-oracle cases, $M \neq O$, we take the worst p_s among all obtained p_s from different marked items.

We obtain [Table 1](#), which shows the size of the network for every operator in $\mathcal{B}_{w, \tau}$, for all unique database sets $w \in \mathcal{D}$, and for all valid marked items, where $\delta = 10^{-4}$. We obtain $\varepsilon \leq 4.8 \times 10^{-11}$ for preparation blocks and $\varepsilon_b \leq 2.5 \times 10^{-8}$ for other blocks. The complete tables that show values of success probabilities p_s are shown in the Appendix, ([Table 3](#)). While this does not complete our analysis of the three-qubit Grover algorithms, these preliminary calculations indicate that the most efficient network will be achieved for $N = 6$ and $w = 012345$ (and not the smaller $N = 5$).

At this point, we complete the classical processing stage of [Algorithm 1](#). Since the blocks are prepared independently, this result can be adapted to develop the full BOQC scheme. However, for $N < 8$, the straightforward implementation of the oracles would require different network sizes for different marked items τ . This would allow Bob to learn about Alice's request to Oscar. In the next section, we complete our exact quantum search algorithm, taking care that networks of identical structure are created for each value of τ , assuring the blindness of the protocol.

3.3 The exact quantum search algorithm with blind oracles

Here we introduce an algorithm called *blind exact quantum search algorithm* (BEQS), given in [Algorithm 3](#), which is an improvement of the Grover-Høyer algorithm: it is compatible with the BOQC scheme, and it involves a general scheme for storing information in the database. Achieving the first means obtaining identical oracles for all marked

Algorithm 3 Blind exact quantum search

Require: n, w, τ, M_{POVM}

(1.a) Classical processing done by Alice

- 1: Prepare $\{\mathcal{A}, \mathcal{D}(\pi), \mathcal{D}(\psi)\}$ (Equation 3) using Algorithm 2, with objective functions f_a or f_b (Equation 11).

(1.b) Classical processing done by Oscar

- 2: Search for the blind oracles $\tilde{\mathcal{O}}$ using Algorithm 2 with the objective function

$$\text{OBJPOVM}(G_j, M_{POVM}, \vec{\varphi}, n, m, w, A, D(\pi), D(\psi)),$$

defined in Subroutine 1, where G_j is the tested network, $\vec{\varphi} \equiv (\vec{\varphi}_1, \dots, \vec{\varphi}_N)$ is the optimization parameters — with random initialization — for all marked items $\tau \in w$, M_{POVM} is the defined POVM, and the rest $(n, m, w, A, D(\pi), D(\psi))$ are defined as those in Algorithm 1. If the optimization succeeds, set $\tilde{\mathcal{O}} \leftarrow G_j$ and $\vec{\varphi}$ is optimized. All oracles now have the same networks, but different parameters, which are set according to the marked item.

- 3: Set $\mathcal{O}(\pi) \leftarrow \tilde{\mathcal{O}}$ and $\mathcal{O}(\varphi + u) \leftarrow \tilde{\mathcal{O}}$; the two oracle calls labelled $\mathcal{O}(\pi)$ and $\mathcal{O}(\varphi + u)$ in previous algorithms will be accomplished by the same oracle operation $\tilde{\mathcal{O}}$.

(2) Quantum processing

- 4: Perform the quantum processing of Algorithm 1 within the respective scheme. If the scheme is BOQC, run it according to the scheme of Figure 1.
 - 5: **Exit**
-

items, whose measurement angles are adjusted accordingly. The latter means permitting several marked items τ to stand for a single database entry; we do this by making the final measurement of the Grover algorithm an incomplete or POVM measurement. For

Subroutine 1 Objective function based on POVM

- 1: **function** OBJPOVM($G_j, M_{POVM}, \vec{\varphi}, n, m, w, A, D(\pi), D(\psi)$)
 - 2: $ov \leftarrow 0$, the objective value
 - 3: **for** τ in w **do**
 - 4: $S \leftarrow G_j(\vec{\varphi}_\tau)$
 - 5: $|\Psi\rangle \leftarrow A|0\rangle^{\otimes n}$
 - 6: **for** $i = 1$ to m **do**
 - 7: $|\Psi\rangle \leftarrow D(\pi)S|\Psi\rangle$
 - 8: **end for**
 - 9: $|\Psi\rangle \leftarrow D(\psi)S|\Psi\rangle$
 - 10: $ov \leftarrow ov + 1 - |\langle \tau | M_{POVM}(\tau) | \Psi \rangle|$
 - 11: $ov \leftarrow ov + |f_{obd}|$ (Equation 12)
 - 12: **end for**
 - 13: **return** ov
 - 14: **end function**
-

instance, consider 2-bit Grover algorithm with database $w = 0123$, $N = 4$, and database entries $\{A, B\}$ ($\tilde{N} = 2$). Note that here we distinguish between the database size (N) and the number of database entries (\tilde{N}). Alice and Oscar agree ahead of time that either outcome 0 or 1 correspond to entry A, and outcome 2 or 3 correspond to entry B; this is attainable by defining measurement operators $\{|0\rangle\langle 0| + |1\rangle\langle 1|, |2\rangle\langle 2| + |3\rangle\langle 3|\}$. We will refer to such a scheme as “POVM measurement strategy”. Physically, it is possible to still do the full projective measurement, then classically associate the measurement outcomes with database entries.

While it is hard analytically to obtain an identical form — in our case using gate networks — of oracles for all marked items, the BEQS provides a numerical method to obtain all those oracles using a single numerical procedure. The key lies in the objective function OBJPOVM in [Subroutine 1](#), which includes two constraints: **(C1)** the success probability must be one, and **(C2)** the resulting operator must preserve the state space. Recall that database choice w induces the state space.

The first constraint, **C1**, implemented at line 10 of [Subroutine 1](#), imposes a successful computation within the defined POVM measurement for all permitted marked items — notice that the loop goes for all $\tau \in w$. Constraint **C2**, implemented at line 11 of [Subroutine 1](#), assures a block diagonal matrix, which is critical when there is a free subspace in the full 2^n -dimensional Hilbert space for an n -qubit system. This constraint is imposed by requiring that the sum of the absolute values of the elements outside diagonal block to be zero:

$$f_{obd} = \sum_{i \in x, j \in x \setminus w, i \neq j} |S_{ij}| + \sum_{i \in x \setminus w, j \in w} |S_{ij}|, \quad (12)$$

where w is the database index, x are all possible indices that can be accommodated, and S is the matrix from evaluating a network $G_j(\vec{\varphi}_\tau)$. All constraints are quantified within the objective value ov . It is worth mentioning that the obtained operator \tilde{O} forms a block diagonal matrix that does necessarily resemble neither the Grover nor the Høyer oracles.

Unfortunately, OBJPOVM requires more resources than f_p and f_b ([Equation 11](#)); therefore for reasons of economy, we set a fixed oracle in every query, which results in fewer optimization parameters. One possible improvement is restricting the legitimate marked items $q \subset w$ to cut the loop at line 3 of [Subroutine 1](#). Returning to the previous example where $w=0123$, $M_{POVM} = \{|0\rangle\langle 0| + |1\rangle\langle 1|, |2\rangle\langle 2| + |3\rangle\langle 3|\}$, and the database entries are $\{A, B\}$, we simply set $q = \{0, 2\}$. Whereas previously Oscar would randomly mark item 0 or 1 to reveal A and would randomly mark 2 or 3 to reveal B, now Oscar marks only 0 to reveal A and marks 2 to reveal B. This amount of speedup resulting from this strategy depends on how small q compared to w .

We test the BEQS for 3-qubit cases, obtaining quantum algorithms within the gate model and the 1WQC model (this takes care of the BOQC model also), where $w = 012345$ and $M_{POVM} = \{|0\rangle\langle 0| + |1\rangle\langle 1|, |2\rangle\langle 2|, |3\rangle\langle 3|, |4\rangle\langle 4|, |5\rangle\langle 5|\}$, thus $N = 6$ and $\tilde{N} = 5$. We choose

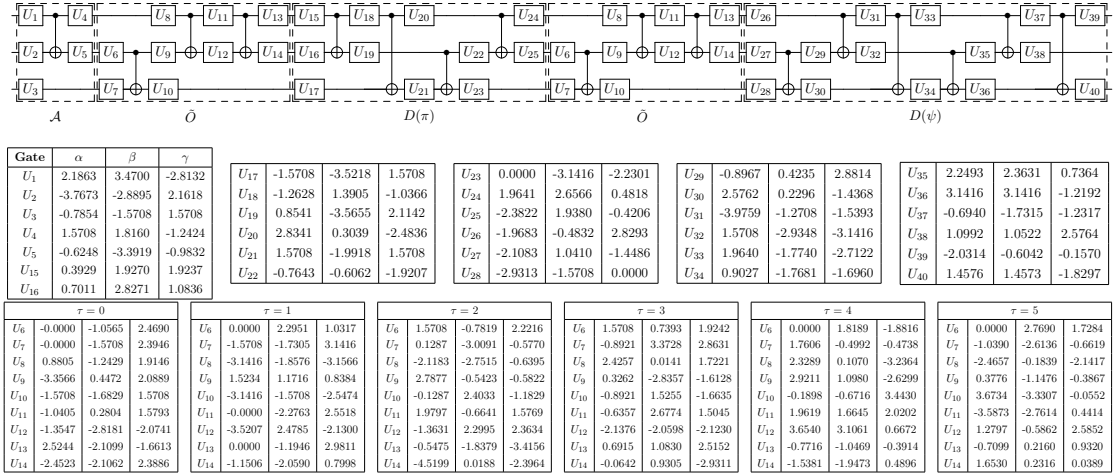


Figure 3: A 3-qubit BEQS (see Algorithm 3) within the gate model for $w = 012345$ and $M_{POVM} = \{|0\rangle\langle 0| + |1\rangle\langle 1|, |2\rangle\langle 2|, |3\rangle\langle 3|, |4\rangle\langle 4|, |5\rangle\langle 5|\}$. Outcomes 0 and 1 refer to the same data, thus $N = 6$ and $\tilde{N} = 5$. The circuit is composed with $\{CNOT, U\}$, where U is a $SU(2)$ matrix and has the form of Equation 6. The parameters for oracles — shown in the tables below — are different for each marked item τ . The circuit has success probabilities $p_s \geq 1 - 10^{-4}$ for all marked items $\tau \in w$.

this configuration based on its potential to result in the smallest gate network based on the study of Table 1. We obtain Figure 3 for the gate model, that is, a circuit comprising $\{CNOT, U\}$, where U has a form of Equation 6. For the BOQC result, we obtain Figure 4. The cluster state is obtained by optimizing networks comprising $\{CPHASE, R_z\}$, where $R_z(\alpha) \equiv e^{-i\alpha Z}$, then transform the result into a graph state, whose measurement angles, along with the α parameters, are the optimization parameters. See Figure 5 for some examples of the correspondence between the gate model and the 1WQC model. In our optimization, we set $\delta = 10^{-4}$ for both models, resulting in precisions $\varepsilon < 2.1 \times 10^{-9}$ for the gate model and $\varepsilon < 1.2 \times 10^{-10}$ for the BOQC model.

We have demonstrated that BEQS obtains exact quantum search algorithms with blind oracles for two computation models. Moreover, BEQS has reduced the size of computation for a five-entry database ($\tilde{N} = 5$) from using 19 CNOT gates (see Table 1) to 17 CNOT gates (see Figure 3). Our work establishes the unfortunate fact that the implementation complexity grows very rapidly for the Grover algorithm in the BOQC model. As a comparison, we obtain a cluster state for the 2-qubit Grover algorithm in Figure 6, where $\tilde{N} = 4$ and $w = 0123$. Going from a four-element database to a five-element database for an exact quantum search algorithm within the BOQC scheme, means going from a 10-node to a 97-node cluster state.

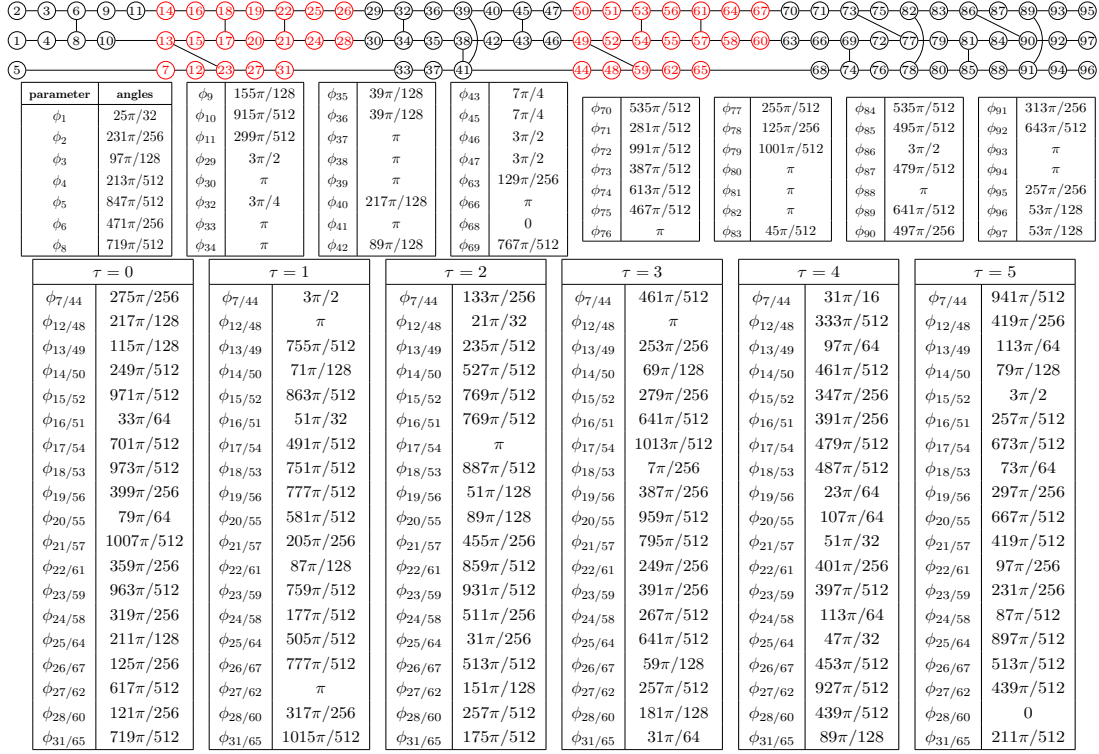


Figure 4: Our 3-qubit BEQS (see [Algorithm 3](#)) for $w = 012345$ and $M_{POVM} = \{|0\rangle\langle 0| + |1\rangle\langle 1|, |2\rangle\langle 2|, |3\rangle\langle 3|, |4\rangle\langle 4|, |5\rangle\langle 5|\}$; thus, $N = 6$ and $\tilde{N} = 5$. Red nodes indicate blind oracles controlled by Oscar, black nodes indicate Alice's computation. The measurement angles, which are specified to 10 bits, for each node is shown in the table; the measurement order is indicated with the node numbers. This computation has success probabilities $p_s \geq 1 - 10^{-4}$ for all queries $\tau \in w$.

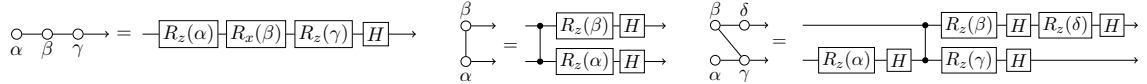


Figure 5: Examples of computation within the gate model and the 1WQC model. The angles below nodes denote measurement angles; measurements are performed from the left to the right. The right hand side of each equation denotes the equivalent computation in the gate model, assuming all measurement outcomes zero.

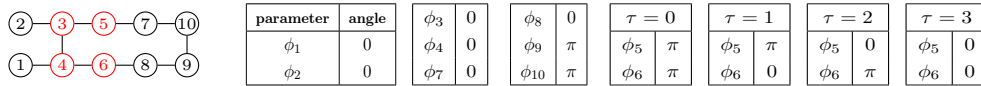


Figure 6: The 2-qubit Grover algorithm within the BOQC scheme, with $N = \tilde{N} = 4$, $w = 0123$, and $M_{POVM} = \{|0\rangle\langle 0|, |1\rangle\langle 1|, |2\rangle\langle 2|, |3\rangle\langle 3|\}$; for notations, follow [Figure 4](#).

3.4 BOQC on NV-centers: the implementation of BEQS algorithms

Here we introduce our proposal to implement a BOQC computation using NV-centers. We propose a direct realization of the results shown above: a physical implementation of 3 qubit BEQS (Figure 4), and of the 2-qubit Grover algorithm (Figure 6). The main challenges for physical implementation are the sizable physical resources — we need 97 qubits to run 3-qubit BEQS — and the high fidelity transmission of encrypted qubits from Alice or Oscar to Bob. We think that these challenges can be at least largely overcome: To deal with the large size, we note the possibility of “reusing” the qubits [24]. To accomplish reliable transmission, we propose using remote state preparation (RSP) [6] as a quantum channel. The re-use strategy drastically decreases the number of qubits: from 97 to 4 qubits for 3-qubit BEQS and from 10 to 3 qubits for 2-qubit Grover. Moreover, RSP is understood to be very efficient for the family of states to be transmitted [32]; for RSP in our setting no additional classical communication at all is needed, automatically maintaining the blindness of the scheme.

For the BOQC implementations that we propose, the total graphs together with measurement angles are shown in Figure 4 for 3-qubit BEQS and Figure 6 for the 2-qubit Grover algorithm. Given that Alice and Oscar have successfully shared the key ξ , and all parties agreed upon a total ordering and graphs, they thus run the protocol shown in Figure 7. In this implementation, the BOQC protocol (see Figure 1) is optimized to perform the computations per partition. Moreover, every partition is divided into smaller subgraphs with size four (three for 2-qubit Grover). This strategy assumes that measured qubits can reset and reused. Processing a computation of a subgraph is described as steps ①–④ in Figure 7. Compared to the UBQC scheme, an additional set of corrections \vec{s} appears as a result from the RSP.

Based on state-of-the-art technologies [26, 29, 14], we estimate the total computation time for 3-qubit BEQS to be 3 seconds, where the time for each step is $t_1 \approx 25$ ms, $t_2 \approx 1.5$ μ s, $t_3 \approx 3.5$ ms, $t_4 \approx 0.5$ ms; assuming every two-bit operation requires 0.5 ms and all the operations on the nuclear spins are performed by coupling the electron spin. For instance, given nuclear spins $\{n_1, n_2\}$ and electron spin e , one applies the CPHASE gate between n_1 and n_2 as follows: SWAP(n_1, e)-CPHASE(e, n_2)-SWAP(n_1, e), where each SWAP gate is implemented with three CNOT gates. For the 2-qubit Grover algorithm, the total run time is estimated to be 305 ms.

Processing one subgraph, that is, executing steps ①–④, requires 1–2 heralded entanglements and 1–2 CPHASE operations, which, on average, is completed within 31 ms for both computations. After measuring a qubit, some qubits are idle until being measured. For the 3-qubit BEQS, the idling qubits need to maintain their coherence for around 91 ms, while around 3 RSPs and other operations are performed on the electron spin. The worst idle case happens at node 23, with idle time 370 ms while 11 RSPs are performed on the electron spin. For the 2-qubit Grover, the idle average is 54 ms, while around 2 RSPs and other operations are performed on the electron spin; the worst idle happens

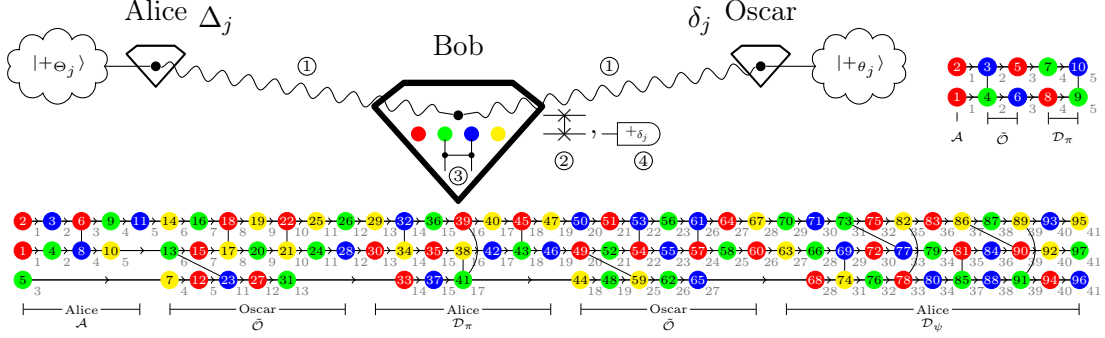


Figure 7: Optimized protocol using three NV-center nodes for the implementation of BOQC. The 97-node graph is the 3-qubit BEQS computation and the 10-node graph is the 2-qubit Grover algorithm. Within the diamonds, the black node represents an electron spin and other colors represent nuclear spins; the node in the graph state will be assigned to the nuclear spin that has the same color. Bob uses his electron spin for multiple purposes: 1) as an interface to create a quantum channel with the clients, 2) as a medium to perform CPHASE gates between nuclear spins, and 3) as an ancilla to measure his nuclear spins. Alice and Oscar alternately control the computation, which comprises $|\mathcal{FG}|$ rounds of steps ①–④ with the ordering shown as node numbers, where \mathcal{FG} is the total graph. The following sequence describes a round of Alice’s moves. ① RSP: Alice and Bob perform a heralded entanglement [3, 7] to share a singlet state $|\Psi^-\rangle = \frac{|01\rangle - |10\rangle}{\sqrt{2}}$ between their two electron spins. Alice has in mind that she wishes to deliver state $|+\Theta_j\rangle$ to Bob. She accomplishes this by measuring her electron spin (i.e., her half of the singlet state) in Θ_j ; depending on her measurement outcome s_j , Bob receives $\frac{|0\rangle + e^{i(\Theta_j + s_j\pi)}|1\rangle}{\sqrt{2}}$, where he knows neither Θ_j nor s_j . ② Bob swaps the electron spin with the nuclear spin according to the color. Bob buffers all the required qubits by repeating steps ①–②, which can also be from Oscar. ③ Bob applies CPHASE gates — connecting the nodes in the graph — according to the subgraph; he connects only the nearest neighbor of the node that he is going to measure. ④ Bob measures qubit j in Δ_j — as instructed by Alice — then announces measurement outcome b_j using a public broadcast channel. The angle Δ_j is computed by Alice taking account all the corrections. The same procedure applies to Oscar for his computations. This process is repeated until all nodes are measured. It is worth mentioning that the grey numbers represent a partial ordering induced by flow, which was computed using an algorithm of [35]. Indeed, the total ordering may be selected arbitrarily as long as the partial ordering is respected.

at node 4, which is 170 ms while 5 RSPs are performed on the electron spin. We observe that the ordering we have shown here is not the optimum strategy from the point of view of the idling. It would be possible to insert some redundant nodes to reduce the idle time.

Nuclear spins on NV-centers have been reported to possess coherence time of more than

1 second, even at room temperature [34, 19]. Moreover, high-fidelity one- and two-bit gates operation on the nuclear spins have been demonstrated [40]. While the coherence time seems sufficient, the activities on the electron spins can decohere the idle nuclear spins, especially during the heralded entanglement attempts. Moreover, our time estimation uses the best rate known of heralded entanglement, with the nodes separated by 2 meters [26]. However, the obtained heralded-entanglement fidelity is still low, hence a distillation scheme would be needed. We conclude that the current technology is still not yet ready to implement the algorithms in Figure 7, but foreseeable improvements would make it possible.

Acknowledgment

We thank Tim Taminiau and Slava Dobrovitski for the insightful discussions about NV-centers, to Tal Mor and Rotem Liss for the discussions about distributed and blind computations, to Barbara Terhals’s group in Delft and to IQI members in Aachen for various discussions. We acknowledge the support of Forschungszentrum Jülich for the access to JURECA and RWTH Aachen for the access to clusters.

References

- [1] Martin Abadi, Joan Feigenbaum, and Joe Kilian. “On hiding information from an oracle”. In: *Proceedings of the nineteenth annual ACM symposium on Theory of computing*. ACM. 1987, pp. 195–203. DOI: [10.1016/0022-0000\(89\)90018-4](https://doi.org/10.1016/0022-0000(89)90018-4).
- [2] MS Anwar et al. “Implementing Grover’s quantum search on a para-hydrogen based pure state NMR quantum computer”. In: *Chemical physics letters* 400.1-3 (2004), pp. 94–97. DOI: [10.1016/j.cplett.2004.10.078](https://doi.org/10.1016/j.cplett.2004.10.078).
- [3] Sean D Barrett and Pieter Kok. “Efficient high-fidelity quantum computation using matter qubits and linear optics”. In: *Physical Review A* 71.6 (2005), p. 060310. DOI: [10.1103/PhysRevA.71.060310](https://doi.org/10.1103/PhysRevA.71.060310).
- [4] Stefanie Barz et al. “Demonstration of Blind Quantum Computing”. In: *Science* 335.6066 (2012), pp. 303–308. DOI: [10.1126/science.1214707](https://doi.org/10.1126/science.1214707).
- [5] Charles H Bennet. “Quantum cryptography: Public key distribution and coin tossing”. In: *Proc. of IEEE Int. Conf. on Comp., Syst. and Signal Proc., Bangalore, India, Dec. 10-12, 1984*. 1984. DOI: [10.1016/j.tcs.2014.05.025](https://doi.org/10.1016/j.tcs.2014.05.025).
- [6] Charles H Bennett et al. “Remote state preparation”. In: *Physical Review Letters* 87.7 (2001), p. 077902. DOI: [10.1103/PhysRevLett.87.077902](https://doi.org/10.1103/PhysRevLett.87.077902).
- [7] Hannes Bernien et al. “Heralded entanglement between solid-state qubits separated by three metres”. In: *Nature* 497.7447 (2013), p. 86. DOI: [10.1038/nature12016](https://doi.org/10.1038/nature12016).

- [8] K-A Brickman et al. “Implementation of Grover’s quantum search algorithm in a scalable system”. In: *Physical Review A* 72.5 (2005), p. 050306. DOI: [10.1103/PhysRevA.72.050306](#).
- [9] Anne Broadbent, Joseph Fitzsimons, and Elham Kashefi. “Universal blind quantum computation”. In: *Foundations of Computer Science, 2009. FOCS’09. 50th Annual IEEE Symposium on*. IEEE. 2009, pp. 517–526. DOI: [10.1109/FOCS.2009.36](#).
- [10] Kai Chen et al. “Experimental realization of one-way quantum computing with two-photon four-qubit cluster states”. In: *Physical review letters* 99.12 (2007), p. 120503. DOI: [10.1103/PhysRevLett.99.120503](#).
- [11] Dong Pyo Chi and Jinsoo Kim. “Quantum database search by a single query”. In: *Lecture notes in computer science* (1999), pp. 148–151. DOI: [10.1007/3-540-49208-9_11](#).
- [12] Isaac L Chuang, Neil Gershenfeld, and Mark Kubinec. “Experimental implementation of fast quantum searching”. In: *Physical review letters* 80.15 (1998), p. 3408. DOI: [10.1103/PhysRevLett.80.3408](#).
- [13] Richard Cleve et al. “Quantum entanglement and the communication complexity of the inner product function”. In: *Quantum Computing and Quantum Communications*. Springer, 1999, pp. 61–74. DOI: [10.1007/3-540-49208-9_4](#).
- [14] Julia Cramer et al. “Repeated quantum error correction on a continuously encoded qubit by real-time feedback”. In: *Nature communications* 7 (2016), p. 11526. DOI: [10.1038/ncomms11526](#).
- [15] Vincent Danos and Elham Kashefi. “Determinism in the one-way model”. In: *Physical Review A* 74.5 (2006), p. 052310. DOI: [10.1103/PhysRevA.74.052310](#).
- [16] Shantanu Debnath et al. “Demonstration of a small programmable quantum computer with atomic qubits”. In: *Nature* 536.7614 (2016), p. 63. DOI: [10.1038/nature18648](#).
- [17] L DiCarlo et al. “Demonstration of two-qubit algorithms with a superconducting quantum processor”. In: *Nature* 460.7252 (2009), p. 240. DOI: [10.1038/nature08121](#).
- [18] David P DiVincenzo and John Smolin. “Results on two-bit gate design for quantum computers”. In: *Proceedings of the Workshop on Physics and Computation, PhysComp ’94*. eprint arXiv: cond-mat/9409111. IEEE Press, 1994, p. 14. DOI: [10.1109/PHYCMP.1994.363704](#).
- [19] Florian Dolde et al. “Room-temperature entanglement between single defect spins in diamond”. In: *Nature Physics* 9.3 (2013), p. 139. DOI: [10.1126/science.1220513](#).
- [20] Mang Feng. “Grover search with pairs of trapped ions”. In: *Physical Review A* 63.5 (2001), p. 052308. DOI: [10.1103/PhysRevA.63.052308](#).
- [21] C Figgatt et al. “Complete 3-qubit Grover search on a programmable quantum computer”. In: *Nature communications* 8.1 (2017), p. 1918. DOI: [10.1038/s41467-017-01904-7](#).

- [22] Cica Gustiani and David P DiVincenzo. “Blind Oracular Quantum Computation”. unpublished. N.D.
- [23] Bas Hensen et al. “Loophole-free Bell inequality violation using electron spins separated by 1.3 kilometres”. In: *Nature* 526.7575 (2015), p. 682. DOI: [10.1038/nature15759](https://doi.org/10.1038/nature15759).
- [24] Monireh Houshmand, Mahboobeh Houshmand, and Joseph F. Fitzsimons. “Minimal qubit resources for the realization of measurement-based quantum computation”. In: *Phys. Rev. A* 98 (1 2018), p. 012318. DOI: [10.1103/PhysRevA.98.012318](https://doi.org/10.1103/PhysRevA.98.012318).
- [25] Peter Høyer. “Arbitrary phases in quantum amplitude amplification”. In: *Phys. Rev. A* 62 (5 2000), p. 052304. DOI: [10.1103/PhysRevA.62.052304](https://doi.org/10.1103/PhysRevA.62.052304).
- [26] Peter C Humphreys et al. “Deterministic delivery of remote entanglement on a quantum network”. In: *Nature* 558.7709 (2018), p. 268. DOI: [10.1038/s41586-018-0200-5](https://doi.org/10.1038/s41586-018-0200-5).
- [27] Eric Jones, Travis Oliphant, Pearu Peterson, et al. *SciPy: Open source scientific tools for Python*. <http://www.scipy.org>. Accessed: 2018-06-25. 2001–.
- [28] Jonathan A Jones, Michele Mosca, and Rasmus H Hansen. “Implementation of a quantum search algorithm on a quantum computer”. In: *Nature* 393.6683 (1998), p. 344. DOI: [10.1038/30687](https://doi.org/10.1038/30687).
- [29] Norbert Kalb et al. “Entanglement distillation between solid-state quantum network nodes”. In: *Science* 356.6341 (2017), pp. 928–932. DOI: [10.1126/science.aan0070](https://doi.org/10.1126/science.aan0070).
- [30] Yang Liu. “An exact quantum search algorithm with arbitrary database”. In: *International Journal of Theoretical Physics* 53.8 (2014), pp. 2571–2578. DOI: [10.1007/s10773-014-2055-3](https://doi.org/10.1007/s10773-014-2055-3).
- [31] Yang Liu and FeiHao Zhang. “First experimental demonstration of an exact quantum search algorithm in nuclear magnetic resonance system”. In: *Science China Physics, Mechanics & Astronomy* 58.7 (2015), pp. 1–6. DOI: [10.1007/s11433-015-5661-z](https://doi.org/10.1007/s11433-015-5661-z).
- [32] Hoi-Kwong Lo. “Classical-communication cost in distributed quantum-information processing: A generalization of quantum-communication complexity”. In: *Phys. Rev. A* 62 (1 2000), p. 012313. DOI: [10.1103/PhysRevA.62.012313](https://doi.org/10.1103/PhysRevA.62.012313).
- [33] Gui-Lu Long. “Grover algorithm with zero theoretical failure rate”. In: *Physical Review A* 64.2 (2001), p. 022307. DOI: [10.1103/PhysRevA.64.022307](https://doi.org/10.1103/PhysRevA.64.022307).
- [34] Peter Christian Maurer et al. “Room-temperature quantum bit memory exceeding one second”. In: *Science* 336.6086 (2012), pp. 1283–1286. DOI: [10.1126/science.1220513](https://doi.org/10.1126/science.1220513).
- [35] Mehdi Mhalla and Simon Perdrix. “Finding optimal flows efficiently”. In: *International Colloquium on Automata, Languages, and Programming*. Springer. 2008, pp. 857–868. DOI: [10.1007/978-3-540-70575-8_70](https://doi.org/10.1007/978-3-540-70575-8_70).

- [36] Michael A Nielsen. “Cluster-state quantum computation”. In: *Reports on Mathematical Physics* 57.1 (2006), pp. 147–161. DOI: [10.1016/S0034-4877\(06\)80014-5](#).
- [37] WH Press et al. “Numerical Recipes (Cambridge, Univ. Press, Cambridge)”. In: (1986).
- [38] Robert Raussendorf and Hans J. Briegel. “A One-Way Quantum Computer”. In: *Phys. Rev. Lett.* 86 (22 2001), pp. 5188–5191. DOI: [10.1103/PhysRevLett.86.5188](#).
- [39] Robert Raussendorf, Daniel E Browne, and Hans J Briegel. “Measurement-based quantum computation on cluster states”. In: *Physical review A* 68.2 (2003), p. 022312. DOI: [10.1103/PhysRevA.68.022312](#).
- [40] Tim Hugo Taminiau et al. “Universal control and error correction in multi-qubit spin registers in diamond”. In: *Nature nanotechnology* 9.3 (2014), p. 171. DOI: [10.1038/nnano.2014.2](#).
- [41] Lieven M. K. Vandersypen et al. “Implementation of a three-quantum-bit search algorithm”. In: *Applied Physics Letters* 76.5 (2000), pp. 646–648. DOI: [10.1063/1.125846](#).
- [42] Guifre Vidal and Christopher M Dawson. “Universal quantum circuit for two-qubit transformations with three controlled-NOT gates”. In: *Physical Review A* 69.1 (2004), p. 010301. DOI: [10.1103/PhysRevA.69.010301](#).
- [43] Philip Walther et al. “Experimental one-way quantum computing”. In: *Nature* 434.7030 (2005), p. 169. DOI: [10.1038/nature03347](#).
- [44] Stephen Wiesner. “Conjugate Coding”. In: *SIGACT News* 15.1 (Jan. 1983), pp. 78–88. DOI: [10.1145/1008908.1008920](#).
- [45] WL Yang, CY Chen, and M Feng. “Implementation of three-qubit Grover search in cavity quantum electrodynamics”. In: *Physical Review A* 76.5 (2007), p. 054301. DOI: [10.1103/PhysRevA.76.054301](#).
- [46] SHEN Yao, Ai Qing, and Long Gui-Lu. “A Scheme for Simulation of Quantum Gates by Abelian Anyons”. In: *Communications in Theoretical Physics* 56.5 (2011), p. 873. DOI: [10.1088/0253-6102/56/5/13](#).
- [47] Christof Zalka. “Grover’s quantum searching algorithm is optimal”. In: *Physical Review A* 60.4 (1999), p. 2746. DOI: [10.1103/PhysRevA.60.2746](#).

A Appendix

A.1 The arbitrary step of search iteration

This section supplements [Section 2.2](#), namely finding the angles ψ, φ of the Høyer amplitude amplification within the operator $Q(\psi, \varphi)$ [\[25\]](#). Whereas in the Grover algorithm one iteration is restricted to the rotation by $2\theta_0$, the Høyer amplitude amplification allows a rotation within the range $[-2\theta_0, 2\theta_0]$, where θ_0 is the initial angle.

Suppose that we employ n qubits and start with an equal superposition of N basis states $|\Psi_{init}\rangle$ where $2^{n-1} \leq N \leq 2^n$. Let x be the indices that can be realized by n qubits, $x = \{0, \dots, 2^n - 1\}$ and W be a set of all possible subsets of the N -element database, $D = \{w \subseteq x : \|w\| = N\}$, and let $w \in W$, then

$$|\Psi_{init}\rangle = \frac{1}{\sqrt{N}} \sum_{j \in w} |j\rangle. \quad (13)$$

Assume that we have an oracle that implements some function f that can distinguish whether a state is the target. Let y be the set of targets, the action of f be

$$f(j) = \begin{cases} 1, & \text{if } j \in y \\ 0, & \text{if } j \in x \setminus y. \end{cases} \quad (14)$$

The function f induces a subspace spanned by “good state” $|\Psi_1\rangle = \frac{1}{\sqrt{N}} \sum_{\{j:f(j)=1\}} |j\rangle$ and “bad state” $|\Psi_0\rangle = \frac{1}{\sqrt{N}} \sum_{\{j:f(j)=0\}} |j\rangle$. Thus, the initial state can be rewritten as $|\Psi_{init}\rangle = |\Psi_1\rangle + |\Psi_0\rangle$. Let us search for M targets. In the normalized basis of good and bad states, we rewrite again the initial state

$$|\Psi_{init}\rangle = \sqrt{a} |\tilde{\Psi}_1\rangle + \sqrt{1-a} |\tilde{\Psi}_0\rangle \quad (15)$$

where $|\tilde{\Psi}_1\rangle = \frac{1}{\sqrt{M}} |\Psi_1\rangle$, $|\tilde{\Psi}_0\rangle = \frac{1}{\sqrt{N-M}} |\Psi_0\rangle$, and $a = \frac{M}{N} \equiv \sin^2(\theta_0)$.

Let $Q(\varphi, \psi)$ be the operator that performs search iteration with parameters $\varphi, \psi \in [0, 2\pi)$

$$Q(\varphi, \psi) \equiv -\mathcal{A}S_0(\psi)\mathcal{A}S_y(\varphi). \quad (16)$$

Where \mathcal{A} is the preparation operator that transforms state $|0\rangle^{\otimes n}$ into the equal superposition state $\mathcal{A}|0\rangle^{\otimes n} = |\Psi_{init}\rangle$. In the Grover algorithm of database size 2^n , \mathcal{A} basically consists of Hadamards. Note that we can prepare $|\Psi_{init}\rangle$ from any convenient starting state. For simplicity, we start with zero state $|0\rangle^{\otimes n}$.

Essentially, $Q(\varphi, \psi)$ consists of one oracle call $S_y(\varphi)$ and a diffusion operator $D(\psi) \equiv \mathcal{A}S_0(\psi)\mathcal{A}$. The oracle call $S_y(\varphi)$ “marks” the targets y by $e^{i\varphi}$ and it can be defined as

$$S_y(\varphi) := I - (1 - e^{i\varphi}) |\tilde{\Psi}_1\rangle \langle \tilde{\Psi}_1|. \quad (17)$$

The operator $S_0(\psi)$ marks the state before preparation (in our case was $|0\rangle^{\otimes n}$) with phase $e^{i\psi}$. Thus, the diffusion operator follows

$$D(\psi) = \mathcal{A} \left[I - (1 - e^{i\psi}) (|0\rangle \langle 0|)^{\otimes n} \right] \mathcal{A} = I - (1 - e^{i\psi}) |\Psi_{init}\rangle \langle \Psi_{init}|. \quad (18)$$

By using basis $\{|\tilde{\Psi}_0\rangle, |\tilde{\Psi}_1\rangle\}$, we can represent Q in matrix form

$$Q(\varphi, \psi) = \begin{bmatrix} -a(1 - e^{i\psi}) - e^{i\psi} & (1 - e^{i\psi})e^{i\varphi}\sqrt{a(1-a)} \\ (1 - e^{i\psi})\sqrt{a(1-a)} & a(1 - e^{i\psi})e^{i\varphi} - e^{i\varphi} \end{bmatrix}. \quad (19)$$

Now, the question is: how to implement an arbitrary rotation θ from $|\Psi_{init}\rangle$ by applying $Q(\varphi, \psi)$? We need to find out what are φ and ψ given θ . By imposing some conditions on φ and ψ , we can find them by using some tricks.

Note that we are only working with two dimensional Hilbert space spanned by the complex vectors $\{|\tilde{\Psi}_0\rangle, |\tilde{\Psi}_1\rangle\}$. Therefore, we may associate Q with some general form of two-dimensional unitary operator.

Given an arbitrary unitary operator U with four parameters $\delta, \varphi_1, \varphi_2, \theta \in [0, 2\pi)$

$$U = e^{i\frac{\delta}{2}} \begin{pmatrix} e^{i\varphi_1} \cos(\theta) & e^{i\varphi_2} \sin(\theta) \\ -e^{i\varphi_2} \sin(\theta) & e^{-i\varphi_1} \cos(\theta) \end{pmatrix}. \quad (20)$$

Let us transform the parameters into the following. Let $\varphi_1 = \mu + \nu$ and $\varphi_2 = \mu - \nu + \pi$, thus

$$U = e^{i\frac{\delta}{2}} \begin{pmatrix} e^{i\mu+i\nu} \cos(\theta) & -e^{i\mu-i\nu} \sin(\theta) \\ e^{i\mu-i\nu} \sin(\theta) & e^{-i\mu-i\nu} \cos(\theta) \end{pmatrix}. \quad (21)$$

We impose the condition that the diagonal elements be equal; that is fulfilled if and only if $\varphi_1 = -\varphi_1$. This implies $\varphi_1 = 0$ and thus $\nu = -\mu$. Let us call this matrix \tilde{U} . Latter, we re-parameterize \tilde{U} by setting $\delta/2 = v$ and $2\mu = u$, thus

$$\tilde{U} = e^{i\frac{\delta}{2}} \begin{pmatrix} \cos(\theta) & -e^{i2\mu} \sin(\theta) \\ e^{-i2\mu} \sin(\theta) & \cos(\theta) \end{pmatrix} = e^{iv} \begin{pmatrix} \cos(\theta) & -e^{iu} \sin(\theta) \\ e^{-iu} \sin(\theta) & \cos(\theta) \end{pmatrix}. \quad (22)$$

We factorize \tilde{U} in the following way:

$$\tilde{U} = e^{iv} \begin{pmatrix} 1 & 0 \\ 0 & e^{-iu} \end{pmatrix} \begin{pmatrix} \cos(\theta) & -\sin(\theta) \\ \sin(\theta) & \cos(\theta) \end{pmatrix} \begin{pmatrix} 1 & 0 \\ 0 & e^{iu} \end{pmatrix}. \quad (23)$$

In this form, it is easy to see that \tilde{U} performs a real rotation up to some conditional phases. The aim is to associate our search operator Q with \tilde{U} .

We set Q such that its diagonal elements are also equal, which means $-a(1 - e^{i\psi}) - e^{i\psi} = a(1 - e^{i\psi})e^{i\varphi} - e^{i\varphi}$. From the Høyer's result [25], suppose $\varphi \neq \pi$, then this condition is fulfilled if and only if

$$\tan(\varphi/2) = \tan(\psi/2)(1 - 2a). \quad (24)$$

Given \tilde{Q} , which is the matrix Q with equal diagonal elements. At this point, it is straightforward to parameterize \tilde{Q} . We can find parameters ψ and φ in the following manner

$$\begin{aligned} \left\| (1 - e^{i\psi})\sqrt{a(1-a)} \right\| &= \sin(\theta) \\ \psi &= \arccos \left(1 - \frac{\sin^2(\theta)}{2a(1-a)} \right) \end{aligned} \quad (25)$$

$$\varphi = 2 \arctan(\psi/2)(1 - 2a). \quad (26)$$

Now we are able to perform an arbitrary rotation θ on a state $|\Psi_{init}\rangle$ with initial angle $\theta_0 = \arcsin(\sqrt{a})$ using $\tilde{Q}(\varphi, \psi)$, up to some conditional phases. Thus, we may relate Q and \tilde{Q} by canceling its conditional phases

$$Q = e^{-iv} \begin{pmatrix} 1 & 0 \\ 0 & e^{iu} \end{pmatrix} \tilde{Q} \begin{pmatrix} 1 & 0 \\ 0 & e^{-iu} \end{pmatrix}. \quad (27)$$

Two additional parameters are necessary in order to have a correct rotation, thus $Q = Q(\varphi, \psi, u, v)$. By knowing ψ , the phases u and v can be obtained straightforwardly, for instance

$$v = \arg \left(-a(1 - e^{i\psi}) - e^{i\psi} \right) \quad (28)$$

$$u = v - \arg \left((1 - e^{i\psi}) \sqrt{a(1 - a)} \right). \quad (29)$$

Since one rotation is limited to $\theta \in [-2\theta_0, 2\theta_0]$, we need to split it into several iterations if $\|\theta\| > \|2\theta\|$. Suppose we perform $m > 1$ iterations for which each iteration rotates $\tilde{\theta} = \theta/m$ with parameters \tilde{u}, \tilde{v} , thus

$$Q^m = e^{-im\tilde{v}} \begin{pmatrix} 1 & 0 \\ 0 & e^{i\tilde{u}} \end{pmatrix} \begin{pmatrix} \cos(\tilde{\theta}) & -\sin(\tilde{\theta}) \\ \sin(\tilde{\theta}) & \cos(\tilde{\theta}) \end{pmatrix}^m \begin{pmatrix} 1 & 0 \\ 0 & e^{-i\tilde{u}} \end{pmatrix}. \quad (30)$$

For the identical iterations, the phase corrections need only be performed once at the beginning and end, since they will be canceled out in the intermediate stages.

A.2 The exhaustive search circuit

N	Equivalent combinations of database
5	01234, 01235, 01236, 01237, 01245, 01246, 01345, 01357, 01456, 01457, 02346, 02367, 02456, 02467, 04567, 12357, 12367, 13457, 13567, 14567, 23467, 23567, 24567, 34567
	01247, 01356, 02356, 03456, 03567, 12347, 12457, 12467
	01256, 01257, 01267, 01346, 01347, 01367, 01467, 01567, 02345, 02347, 02357, 02457, 02567, 03457, 03467, 12345, 12346, 12356, 12456, 12567, 13456, 13467, 23456, 23457
6	012345, 012346, 012357, 012367, 012456, 013457, 014567, 023467, 024567, 123567, 134567, 234567
	012567, 013467, 023457, 123456
	012347, 012356, 012457, 012467, 013456, 013567, 023456, 023567, 034567, 123457, 123467, 124567
7	0123456, 0123457, 0123467, 0123567, 0124567, 0134567, 0234567, 1234567
8	01234567

Table 2: The equivalent combination of database for each N . The equivalent combinations are listed within the same row.

(a) $N=5, \zeta + \varphi=1.7076, \psi=0.4510, w=01234$

	\mathcal{A}	$O(\pi)$					$D(\pi)$	$O(u + \varphi)$					$D(\psi)$
CNOT		0	1	2	3	4		0	1	2	3	4	
0	0.7449	0.3463	0.8592	0.5187	0.8197	0.4388	0.2380	0.4388	0.8428	0.4449	0.8375	1.0000	0.9604
1	0.8575	1.0000	0.8062	1.0000	0.6723	1.0000	0.3114	1.0000	0.6790	1.0000	0.7084		0.9236
2	1.0000		1.0000		1.0000		0.5350		1.0000		1.0000		0.9525
3							0.7062						0.9329
4							0.7715						0.9845
5							0.8948						0.9832
6							0.9781						0.9973
7							0.9999						0.9990
8							1.0000						0.9999
9													1.0000

(b) $N=5, \zeta + \varphi=1.7076, \psi=0.4510, w=01247$

	\mathcal{A}	$O(\pi)$					$D(\pi)$	$O(u + \varphi)$					$D(\psi)$
CNOT		0	1	2	4	7		0	1	2	4	7	
0	0.6500	1.0000	0.8006	0.5706	0.9271	0.5950	0.2233	0.5950	0.9507	0.6047	0.9005	0.6313	0.9446
1	0.6581		0.9647	1.0000	0.7872	1.0000	0.1646	1.0000	0.7268	1.0000	0.7588	1.0000	0.3315
2	1.0000		1.0000		1.0000		0.3310		1.0000		1.0000		0.9543
3							0.4529						0.8952
4							0.6318						0.9766
5							0.7458						0.9731
6							0.9251						0.9912
7							1.0000						0.9979
8													0.9999

(c) $N = 5, \zeta + \varphi = 1.7076, \psi = 0.4510, w = 01256$

	\mathcal{A}	$O(\pi)$					$D(\pi)$	$O(u + \varphi)$					$D(\psi)$
CNOT		0	1	2	5	6		0	1	2	5	6	
0	0.6542	1.0000	1.0000	0.3625	0.8350	0.3108	0.2221	0.3108	0.8432	0.4082	0.8533	0.2448	0.9604
1	0.8575			1.0000	0.7236	1.0000	0.2538	1.0000	0.6802	1.0000	0.6979	1.0000	0.9279
2	0.9397				1.0000		0.3660		1.0000		1.0000		0.9717
3	1.0000						0.5617						0.8967
4	0.8184						0.7715						0.9778
5	0.9326						0.8026						0.9835
6	0.9482						0.9293						0.9979
7	1.0000						0.9996						0.9986
8							1.0000						0.9998
9													0.9999

(d) $N = 6, \zeta + \varphi = 1.8605, \psi = 0.8411, w = 012345$

	\mathcal{A}	$O(\pi)$					$D(\pi)$	$O(u + \varphi)$					$D(\psi)$		
CNOT		0	1	2	3	4	5		0	1	2	3	4	5	
0	0.8024	0.3570	0.9079	0.3721	0.7899	0.4035	0.7407	0.2733	0.7407	0.3683	0.8720	0.3966	0.8621	0.2421	0.9248
1	1.0000	0.3702	0.6940	0.4278	0.7054	1.0000	0.6414	0.1892	0.6414	1.0000	0.6663	1.0000	0.6932	1.0000	0.8756
2		1.0000	0.6434	1.0000	0.6617		1.0000	0.6892	1.0000		1.0000		1.0000		0.9077
3			0.7156		0.7156			0.8268							0.8481
4			1.0000		1.0000			1.0000							0.9698
5								1.0000							0.9806
6															1.0000

(e) $N = 6, \zeta + \varphi = 1.8605, \psi = 0.8411, w = 012347$

	\mathcal{A}	$O(\pi)$						$D(\pi)$	$O(u + \varphi)$						$D(\psi)$
		0	1	2	3	4	7		0	1	2	3	4	7	
CNOT															
0	0.7714	0.3917	0.6254	0.3942	0.8433	0.3907	0.8684	0.2694	0.8684	0.4236	0.6345	0.4249	0.8374	0.4950	0.8914
1	0.8024	0.5393	0.6601	1.0000	0.8211	1.0000	0.7526	0.3086	0.7526	0.5410	0.6788	1.0000	0.6773	1.0000	0.1893
2	1.0000	1.0000	0.5921		1.0000		1.0000	0.5476	1.0000	1.0000	0.5958		1.0000		0.9077
3			0.7175					0.6324			0.7258				0.8295
4			1.0000					0.7424			1.0000				0.9641
5								0.8726							0.9641
6								1.0000							0.9824
7															1.0000

(f) $N = 6, \zeta + \varphi = 1.8605, \psi = 0.8411, w = 012567$

	\mathcal{A}	$O(\pi)$						$D(\pi)$	$O(u + \varphi)$						$D(\psi)$
		0	1	2	5	6	7		0	1	2	5	6	7	
CNOT															
0	0.7500	0.2580	0.7261	0.2841	0.7444	0.4075	0.7368	0.1925	0.7368	0.2322	0.7099	0.3807	0.7493	0.3878	0.9251
1	0.7714	1.0000	0.7025	1.0000	0.7219	1.0000	0.7394	0.3731	0.7394	1.0000	0.7227	1.0000	0.7042	1.0000	0.4771
2	0.8293		1.0000		1.0000		1.0000	0.2278	1.0000		1.0000		1.0000		0.8899
3	1.0000							0.2181							0.9037
4								0.6049							0.9617
5								0.6229							0.9631
6								0.8257							0.9813
7								0.9596							0.9996
8								1.0000							0.9999

(g) $N = 7, \zeta + \varphi = 2.0277, \psi = 1.2056, w = 0123456$

	\mathcal{A}	$O(\pi)$						$D(\pi)$	$O(u + \varphi)$						$D(\psi)$		
CNOT		0	1	2	3	4	5	6		0	1	2	3	4	5	6	
0	0.8836	0.5210	0.5794	0.0810	0.4744	0.1625	0.7817	0.4387	0.2131	0.4387	0.6534	0.4318	0.6674	0.4507	0.6005	0.3290	0.8685
1	0.8890	0.4903	0.3747	0.4384	0.4728	0.3949	0.4527	1.0000	0.4133	1.0000	0.6564	0.4652	0.4527	1.0000	0.6774	1.0000	0.4798
2	0.9149	0.5569	0.4636	1.0000	0.6999	1.0000	0.7098		0.5111		1.0000	1.0000	0.6985		1.0000		0.8905
3	1.0000	1.0000	0.6879		0.7345		0.7156		0.6613				0.7136				0.8905
4			1.0000		1.0000		0.7825		0.7016				1.0000				0.9282
5							0.9111		0.7621								0.8409
6							1.0000		0.8239								0.9754
7									0.9719								0.9690
8									1.0000								0.9762
9																	1.0000

(h) $N = 8, \zeta + \varphi = 2.2143, \psi = 1.5708, w = 01234567$

	\mathcal{A}	$O(\pi)$								$D(\pi)$	$O(u + \varphi)$								$D(\psi)$
CNOT		0	1	2	3	4	5	6	7		0	1	2	3	4	5	6	7	
0	1.0000	0.6193	0.7487	0.3517	0.2817	0.3698	0.7262	0.5016	0.3434	0.0156	0.3434	0.1804	0.6695	0.5933	0.3568	0.3061	0.2336	0.5389	0.8565
1		0.6296	0.3980	0.1596	0.3178	0.6412	0.3159	0.0864	0.4831	0.7656	0.4831	0.6222	0.5543	0.5685	0.3384	0.1113	0.4132	0.6278	0.6171
2		0.5042	0.5089	0.3309	0.5023	0.3055	0.5090	0.6350	0.3895	0.5312	0.3895	0.4382	0.3703	0.6321	0.3730	0.6548	0.4884	0.1716	0.8902
3		0.6278	0.7276	0.5495	0.7781	0.5509	0.6162	0.6740	0.7633	0.5312	0.7633	0.5554	0.6200	0.4793	0.6200	0.4275	0.6542	0.7253	0.8902
4		0.5383	0.6945	0.6470	0.7831	0.5704	0.6847	0.4877	0.8043	0.8902	0.8043	0.4531	0.5539	0.6574	0.6994	0.7421	0.6840	0.5769	0.9619
5		0.7407	0.7961	0.7369	0.8875	0.7333	0.8747	0.7372	0.8763	0.8902	0.8763	0.7409	0.8778	0.7286	0.8672	0.7159	0.8760	0.7217	0.9619
6		1.0000	1.0000	1.0000	1.0000	1.0000	1.0000	1.0000	1.0000	1.0000	1.0000	1.0000	1.0000	1.0000	1.0000	1.0000	1.0000	1.0000	1.0000

Table 3: The obtained success probabilities p_s of 3-qubit BEQS; the corresponding column is approximated with an l -size gates network comprises $\{CNOT, U\}$, where U s are 1-qubit unitary gates and l is the number of CNOT gates.